Rheology of magnetofluidized fine powders

M.J. Espin[1], M.A.S. Quintanilla[2], J.M. Valverde[2], A. Castellanos[2]

[1]*Department of Applied Physics II* [2]*Department of Electronics and Electromagnetism.*

University of Seville

Avenida Reina Mercedes s/n, 41012 Sevilla, Spain

(Dated: January 20, 2010)

Abstract

Usually a bed of solid particles fluidized by a gas is inherently unstable. Gas bubbles are rapidly formed at the onset of fluidization, which hinders the efficiency of gas-solid contact. In the case of magnetizable particles, gas bubbles may be suppressed by means of an externally applied field that magnetizes the particles. In general, magnetized particles are assumed to behave as point dipoles that organize in chainlike structures oriented along field lines due to dipole-dipole attraction. The physical mechanism responsible for stabilization is however unclear. In particular, rheological characterization of magnetically stabilized beds (MSBs) has been a subject of controversy and there is not a widely accepted explanation to the empirical fact that magnetofluidized beds can be stabilized by a horizontal field. Several experimental approaches have been used mainly aimed to observe the fluidity of MSBs. Generally, MSBs are reported to behave as a fluid up to a critical magnetic field strength at which the bed is frozen and there appears an appreciable yield stress. Most of these techniques are invasive, which sheds doubts on the mechanism responsible for the apparition of the yield stress. In this work, we have measured the yield stress of MSBs of fine magnetic powders by means of a noninvasive technique that uses gas flow to put the bed under tension. It is shown that the MSB behave as a plastic solid. The yield stress of the stabilized bed, which is developed just at marginal stability, arises as a consequence of the existence of the magnetic attraction between particles at contact. Fine magnetic powders of different aggregative nature have been used in our work. Direct visual observation of mesoscopic structures have revealed that naturally nonaggregated particles organize in quasivertical local linear chains when the field is applied. In contrast, naturally aggregated particles form large-scale branched structures when magnetized by the external field. As a consequence the yield stress of MSBs of naturally aggregated particles is relatively increased and the bed can be stabilized at smaller field intensities. As expected from the attractive force between magnetized particles, the yield stress measured is proportional to the square of the magnetic field intensity, with a proportionality constant that depends on the mesoscopic organization on the magnetic particles. In spite that the magnetic field is applied in the horizontal direction it is shown that quasivertical chainlike structures are stable, which denies the validity of the generally accepted point-dipole model.

I.   INTRODUCTION

Processing and handling of granular materials in fluidized beds is widespread in industry because of their multiple advantages such as enhanced fluid-solid contact and improved flowability. In a typical fluidized bed the material rests on a horizontal porous plate through which fluid is pumped to the granular bed. Granular beds fluidized by gas are however usually unstable, most of the fluid bypassing the bed through large bubbles which curtail uniform expansion and hamper the quality of fluid-solid mixing. As the superficial gas velocity v_g is increased there comes a point at which the gas pressure drop balances the material weight per unit area. At this point the grains become fluidized in a usually heterogeneous state, which is characterized by the rapid development of large gas bubbles rising across the bed. Most commercial gas fluidized bed reactors operate in this state as bubbling fluidized beds. In the bubbling fluidized bed reactor, the upward motion of the gas bubbles enables the mixing of solid particles. However, the bubbles serve as channels for the gases to bypass the solid particles, which hampers the solid-gas contact efficiency [Constantineaua et al. 2007]. Bubbling fluidization is the common behavior found in fluidized beds of coarse granules (typically of size $d_p \gtrsim 100$ μm) as soon as the gas velocity surpasses the minimum fluidization velocity v_{mf}. This type of behavior is the so-called Geldart B behavior according to the Geldart's diagram [Geldart 1973], which was originally derived from empirical observations on beds fluidized by air at ambient conditions. Bubbles can be suppressed in Geldart B beds by artificially enhancing interparticle attractive forces, which otherwise are negligible as compared to particle weight. For example, it has been shown that bubbling beds can be stabilized by incremental addition of a liquid [Seville and Clift 1984] or by fluidizing them with highly adsorbing gases that increase the interparticle attractive force [Xie and Geldart 1995]. According to linear stability analysis, interparticle attractive forces provide the fluidized bed with an effective elastic modulus that may stabilize it against small disturbances [Rietema 1991, Jackson 2001]. In the stably fluidized bed, interparticle contacts become permanently held by the attractive forces. The stabilized bed is thus jammed and takes the appearance of a weak solid [Sundaresan 2003]. When fluidizing finer particles (typically sized between $d_p \simeq 20$ μm and $d_p \sim 50$ μm) the natural van der Waals attractive force between the particles becomes comparable to particle weight. Stable fluidization thus occurs naturally in an interval of gas velocities above minimum fluidization velocity. This is

3

the so-called Geldart A fluidization behavior [Geldart 1973]. From the rheological point of view, stably fluidized beds can be considered as plastic solids. They behave as a solid under low applied stresses and start to flow above a certain level of stress, called the yield stress of the material, which arises as a consequence of the existence of attractive particles between the particles.

A. Magnetostabilization of fluidized beds

Externally applied magnetic fields may stabilize the bubbling fluidization of Geldart B ferromagnetic grains [Johnson and Melcher, Rhodes et al. 2005]. As reviewed by Siegell [Siegell 1989] the earliest reported observation of magnetically stabilized beds dates back to 1960 and was due to Filippov, who observed the behavior of a bubbling bed of iron millimeter-sized particles subjected to an externally imposed magnetic field. Filippov noticed a decrease in particle movement as the strength of the magnetic field was increased until the bed finally reached a stable, calm state. Magnetically stabilized beds (MSBs) yield high solid-gas contact efficiency as a result of their large porosity, which makes them specially suitable for the filtration of pollutants from a gas stream in the continuous operation mode [Melcher 1977, Albert 1985, Cohen and Tien 1991]. It has been shown also that the stable fluidization regime of fluidized beds of fine Geldart A ferromagnetic particles can be further extended to higher gas velocities by imposition of a magnetic field, which makes them very attractive for industrial applications relying on high gas-solid contact efficiency [Valverde et al. 2009].

By extending fluidization linear stability theory to magnetofluidized beds, Rosensweig [Rosensweig 1979b] developed a linear stability analysis that was able to predict that the state of fluidization of magnetic particles could be stabilized against the growth of perturbations in voidage by the action of a magnetic field. Rosensweig assumed the medium to be inviscid, which in most cases is a drastic idealization of the rheological behavior of MSBs, driving him to less-than reliable predictions [Rosensweig 1997]. For example, the analysis predicted that, in the case of magnetic fields applied horizontally (cross-flow configuration), the stability criterion was not satisfied. However, empirical observations demonstrated that magnetic stabilization could be possible for different orientations of the magnetic field, including the cross-flow configuration [Rosensweig 1997, Hristov 1996]. Fur-

ther discrepancies with empirical observations concerned the influence of variables such as particle size [Rosensweig 1997]. A realistic description of magnetostabilized bed rheology is thus an aspect of fundamental relevance to be incorporated into any stability model.

B. Rheology of magnetostabilized beds

Several experimental works have shown that MSBs posses the properties of a plastic solid and can be characterized by a yield stress resulting as the consequence of the magnetic interactions between the particles. Particles in the MSB can flow only when the yield stress is overcome. Rosensweig observations [Rosensweig 1979] indicated that the MSB was free of agitation or solids recirculation, yet it could discharge through an orifice for magnetization fields below a threshold value. Moreover, objects were readily immersed in the bed as in a liquid and a ping-pong ball that was initially rotated continued to spin for several seconds, indicating the low frictional resistance associated with buoyancy. Further experimental studies have shown that the fluidity of MSBs continuously decreases as the magnetic field strength is increased or as the gas fluidization velocity is decreased [Siegell 1988]. Siegell distinguished a transition from the stable to a frozen regime as the field strength was increased above the field strength at marginal stability (H_c) by measuring the ability of the MSB to support high density objects on its surface [Siegell 1988]. For field strengths above a threshold value $H_f > H_c$, the MSB was apparently frozen and objects placed on the bed surface, which had a higher bulk density than the MSB, stood on the surface, indicating a high yield stress. On the other hand, in the non-frozen stabilized bed ($H_c < H < H_f$), higher density objects tended to sink, indicating a negligible yield stress. Accordingly, in the close vicinity of marginal stability, the transfer of the MSB between processing vessels displayed liquidlike features [Siegell 1984]. Tilted bed experiments were another tool used to uphold an apparent transition to a frozen regimes. When a vessel containing a frozen MSB was tilted, the top surface remained normal to the vessel. In contrast, when a vessel containing a non-frozen MSB was tilted, the top surface of the MSB remained horizontal as would a liquid [Siegell 1988].

Lee [Lee 1991] investigated the fluidity of MSBs of coarse magnetite grains by means of solid-discharge tests. His observations indicated that the MSB showed liquidlike behavior for applied fields of strength below a critical value. For field strengths above this so-called

jelling field, the MSB fluidity sharply decreased with increasing field intensity. At a higher field strength the bed was frozen and the solid-discharge rate dropped to zero. Another experimental method consisted of measuring the angle of repose of the solids, which is usually assumed to be related to the yield stress [Siegell 1984]. Due to the attractive interparticle magnetic forces, the MSB became cohesive and its ability to flow decreased with increasing the field strength, which caused an increase of the poured angle of repose.

In spite of the large number of empirical observations on the behavior of magnetofluidized beds, there are few studies reporting a direct measuring method of yield stress. To our knowledge yield stress data has been only reported by Lee [Lee 1983], who designed an invasive technique, which basically consisted of measuring the minimum force needed to pull out a plate from a MSB [Lee 1983]. In these experiments it was observed that a measurable yield stress appeared prominently just at marginal stability and increased monotonically with further increase of the applied field strength. Thus, the distinction between the stabilizing and freezing fields found in many reports seems to depend on the specification of a fluidity based on techniques which are somewhat arbitrary and indirectly related to the yield stress.

In the present work we report experimental data of the tensile yield stress of MSBs of fine magnetic powders by means of a noninvasive experimental technique. Experiments have been performed for fluidized beds of magnetite and steel fine powders stabilized by a cross-flow magnetic field. According to SEM images and previous studies these powders have a distinct aggregative nature in the demagnetized state. Results show that at marginal stability the bed is provided with a measurable yield stress that can be correlated to magnetic field strength and mesoscopic structuring of the particles.

II.   EXPERIMENTAL SETUP AND MATERIALS

The experimental setup to measure the tensile yield stress σ_t of MSBs used in this work is based on the Seville Powder Tester (SPT), whose functioning has been reported in detail elsewhere [Valverde et al. 2000]. The powder sample is held in a vertically oriented cylindrical vessel (2.54cm internal diameter in the experiments reported in this paper) and rests on a porous plate that acts as gas distributor (5μm pore size). By means of a series of computer controlled valves and a mass flow controller, a controlled flow of filtered and dried air is pumped through the powder bed while the gas pressure drop across it is read from a

differential pressure transducer. The height of the bed, which gives an average value of the particle volume fraction ϕ, is measured by means of an ultrasonic sensor placed on top of the vessel. This device can determine distance, with an accuracy smaller than local fluctuations in bed height, by sending an ultrasonic wave and measuring the time of reflection from the target.

The powders used in the experiments are unmagnetized magnetite and steel fine powders artificially made by Xerox Co. Solid densities ρ_p of magnetite and steel particles, measured by means of a AccuPyc 1330 pycnometer, are 5060 kg/m^3 and 7920 kg/m^3, respectively. The behavior of these unmagnetized powders has been extensively studied by a statistical analysis of avalanches in a half-filled and slowly rotated drum [Quintanilla et al. 2004, Quintanilla et al. 2006]. Avalanches mainly consisted of long-range time correlated small avalanches lacking a typical size as typically found for slightly cohesive powders [Quintanilla et al. 2001]. A relevant difference in the behavior of the powders used in the present study concerns the distributions of angle of avalanche and angle of repose, which for the steel powder were wider and shifted to higher values indicating its larger cohesiveness [Quintanilla et al. 2006] as will be seen in this paper from direct measurements of the tensile yield stress. Scanning Electron Microscope photographs of both powders can be seen in Fig. 1, which show a relevant difference of particle morphology. Steel particles are irregularly shaped while, in contrast, magnetite particles are roundly shaped eventhough their surface is rough.

A relevant distinction is the higher presence of fines in the steel powder, which favors particle aggregation and thus the cohesive behavior. Normalized particle size distributions are shown in Fig. 2 obtained by means of laser-based GALAIS CIS-1 analyzer. Number average size are 46 μm for the magnetite powder and 41 μm for the steel powder. Note that, in any case, the size of these particles is large compared to that of particles in colloidal ferrofluids. Thus, unlike in colloidal magnetic fluids, in our magnetofluidized beds particles are multidomain and their Brownian motion is totally negligible.

Our magnetic powders have been tested as affected by a cross-flow uniform magnetic field externally imposed. The strength of the magnetic field is varied by adjusting the electrical current through a pair of square Helmholtz coils (50×50 cm) with each coil consisting of 500 turns of 2 mm dia. copper wire. The magnetic field strength is measured by a Hirst Magnetics Gaussmeter using an axial probe with an accuracy less than 0.1 mT. Experimental

measurements show that, within this experimental accuracy, the external field strength is homogeneous in the cell volume.

The magnetic powders employed in our experiments were not permanently magnetized. Thus, for the small field strengths applied in our work ($H_0 < 5$ kA/m), the magnetic response of the powders should be linear and reversible [Mills 2004]. Particle magnetization $\mathbf{M_p}$ would be therefore related to the externally imposed field $\mathbf{H_0}$ by means of the linear relationship $\mathbf{M_p} = \chi_p \mathbf{H_0}$, where χ_p is the initial particle susceptibility. Mills reported values of the initial susceptibility of natural magnetite about 2.3 for low fields, and always remained $\lesssim 10$ [Mills 2004]. Hunt et al. [Hunt et al. 1995] reviewed plenty of data in the literature for magnetite rocks, which ranged from $\chi_p = 1$ to $\chi_p = 5.7$. Hunt et al. [Hunt et al. 1995] reviewed also data on the initial susceptibility of magnetite particles of size between 0.01 and 100 μm, made from either crushing or crystal growing. The values reported of χ_p ranged between 2.5 and 10. On the other hand, values reported in the literature for the magnetic susceptibility of steel particles are highly dependent on variables such as the presence of additives, carbon content, processing method, etc., and span in a wide range from $\chi_p \sim 1$ to $\chi_p \sim 10^3$ [Bauccio 1994].

Since the data reported in the literature spans in a wide range, a first step of our work has consisted of obtaining χ_p for our experimental particles. This has been accomplished by measuring in our experimental setup the strength of the field at a fixed point (see Fig. 3) with and without the powder bed present. The powder bed is allowed to settle in the cylindrical vessel after being fluidized at a gas velocity $v_g = 2$ cm/s to ensure reproducibility of the packing conditions. For a given current intensity I, the field $\mathbf{H}$ consists of the superposition of the external applied field $\mathbf{H_0}$, which is directed along the x-axis and was previously measured in the absence of the powder bed for the same current intensity, and the field $\mathbf{H_m}$ caused by the magnetized powder bed of height $h \simeq 2$ cm. Upon application of the external field the powder is assumed to be uniformly magnetized with a magnetization $\mathbf{M} = M\mathbf{u_x}$. The strength of the x-component of the field $\mathbf{H_m}$ is calculated numerically as $H_{mx} = 0.039M$ at the point of measurement, which is located at a height $z_0 = 2.4$ cm above the bottom of the bed and at a distance $x_0 = 2.51$ cm from its vertical central axis (see Fig. 3). In Fig. 4 we show data on the bulk magnetization $M = (H_{mx} - H_0)/0.039$ obtained from this procedure. As expected the bulk magnetization changes linearly and reversibly as the strength of the external field H_0 is varied. The data in Fig. 4 can be well fitted by the

equation $M = \chi H_0$, where the bulk susceptibility χ is similar for both powders ($\chi = 1.81$ for the magnetite powder and $\chi = 1.86$ for the steel powder).

According to effective medium theories and numerical analysis on random granular materials [Karkkainen et al. 2001], the bulk susceptibility χ of a bed of magnetically linear spherical particles of susceptibility χ_p located in a homogeneous environment of susceptibility χ_0 can be approximately calculated from the Bruggeman mixing rule

$$(1 - \phi)\frac{\chi_0 - \chi}{3 + \chi_0 + 2\chi} + \phi\frac{\chi_p - \chi}{3 + \chi_p + 2\chi} = 0 \tag{1}$$

where, in our case, $\chi_0 = 0$ and the particle volume fraction is $\phi = 0.48$ for magnetite and $\phi = 0.43$ for steel. From Eq. 1 we obtain the particle susceptibilities $\chi_p = 5.33$ (magnetite) and $\chi_p = 6.71$ (steel), which are in the range of values reported in the literature.

In a previous research we have measured the tensile yield stress of the roundly shaped magnetite powder as affected by application of the magnetic field according to two different operation modes [Valverde et al. 2009]. In the *H off/on* operation mode, the particle bed was driven to bubbling in the absence of magnetic field. Once the gas velocity was decreased below the bubbling onset and the bed was stabilized by the natural cohesive forces alone, the field was applied. In the *H on/on* mode, the field was kept during the whole process of bubbling and stabilization. In this operation mode, the field was the main stabilizing source. It was found that the tensile yield stress of the naturally stabilized bed was not essentially changed by application of the field a posteriori (*H off/on*), which was attributed to the inability of the field to alter the arrangement of the particles once they were jammed in the stable fluidization state. In contrast, when the magnetic field was held on during bubbling and transition to stable fluidization (*H on/on* mode), the tensile yield stress was appreciably increased, which indicated a relevant role of the magnetic field in the arrangement of the particles. In the present work we will focus on the effect of particle aggregation in the absence of magnetic field on the yield stress of magnetically stabilized bed in the *H on/on* mode. For that purpose we will use the naturally aggregated steel particles, which have a similar bulk susceptibility to the mostly individual magnetite particles.

III.   EXPERIMENTAL RESULTS

A.   Tensile yield stress of the naturally stabilized bed

Figure 5 shows data of the gas pressure drop across the powder bed Δp (made nondimensional with the powder weight per unit area W) as a function of the superficial gas velocity v_g and in the absence of magnetic field for both magnetite and steel powders. In these tests, the powder is first driven to the bubbling regime by imposing a gas velocity larger than $v_g = 2$ cm/s. Once the bubbling bed has reached a stationary state, in which it has lost the memory of its previous history [Valverde et al. 2003, Valverde et al. 2001], the gas flow is suddenly turned off and the bed is allowed to settle. The consolidation stress σ_c in this initial state at the bottom of the sample is given by the powder own weight per unit area W. (Since we restrict our study to shallow beds, with heights smaller than bed diameter, wall retention effects can be considered as negligible [Valverde et al. 1998].) The settled powder layer is then subjected to a slowly increasing gas velocity. At first the bed structure is unperturbed and Δp increases linearly as v_g is increased (see Fig. 5). This linear behavior corresponds to Carman's law [Carman 1937] for the resistance of porous solids to the passage of gas flow. The larger the porosity ε, or, equivalently, the smaller the particle volume fraction $\phi = 1 - \varepsilon$, the smaller the slope. This is clearly seen in Fig. 5 in the different initial slopes for the magnetite ($\phi = 0.48$) and steel ($\phi = 0.43$) powders. Δp balances W at the point of minimum fluidization velocity $v_g = v_{mf}$ (see Fig. 5). At this point a powder with zero cohesion would become fluidized, yet the pressure drop across our naturally cohesive powders continues to increase above the minimum fluidization velocity. Above this point the gas flow puts the bed under tension, and as the tension builds up there comes a point at which the powder breaks in tension and the pressure drop falls down to around the weight per unit area W (see Fig. 5). The condition for tensile yield is met first at the bottom of the bed, where the fracture of the bed is observed to start as it is theoretically expected [Castellanos et al. 2004]. Provided that wall effects are negligible, the tensile yield stress σ_t of the settled powder is given by the difference between the pressure drop across the bed just before the breaking and the weight per unit area $\sigma_t = (\Delta p)_{max} - W$, which is $\sigma_t \simeq 45$ Pa for the magnetite powder bed and $\sigma_t \simeq 71$ Pa for the steel powder bed. Further increase of the gas velocity gives rise to a state of heterogeneous fluidization, whose main characteristic

is the propagation of the fracture in the upward direction while Δp fluctuates around the powder weight per unit area and visible bubbles are developed.

If the gas velocity is now decreased from the bubbling regime, the typical hysteretic behavior of Geldart A powders becomes apparent below a gas velocity $v_g = v_c$ at which the fluidized bed is jammed and stabilized. For $v_g = v_0 < v_c$ it is $\Delta p < W$ (see Fig. 5), indicating that part of the weight is sustained by the enduring interparticle contacts. Thus, at a given state in the stable fluidization interval, there exists a consolidation stress σ_c at the bottom of the bed given by $\sigma_c = W - \Delta p_0$, where Δp_0 is the gas pressure drop across the stably fluidized bed for a gas velocity $v_0 < v_c$. At marginal stability ($v_0 = v_c$) it is $\sigma_c = 0$. If the gas flow during the defluidization part of the cycle is increased again from any stably fluidized state at $v_g = v_0$, the behavior becomes again hysteretic and Δp increases linearly as v_g is increased, in agreement with Carman's law (see Fig. 6). The slope of this new straight line is smaller the larger v_0, indicating a larger porosity of the stably fluidized bed as should correspond to higher expansion. Like in the case of the initially settled bed ($v_0 = 0$), a pressure overshoot can be observed for the beds initially settled at $0 < v_0 < v_c$, which enables us to measure the tensile yield stress σ_t of the bed as a function of the reduced consolidation $\sigma_c = W - \Delta p_0$. As can be seen in Fig. 6, the pressure overshoot is smaller as v_0 is increased and becomes inappreciable as v_0 approaches marginal stability.

The measured consolidation stress σ_c and tensile yield stress σ_t of the powder beds are shown as a function of v_0 in Fig. 7. As expected, σ_c and σ_t decrease as v_0 is increased. Within the accuracy of our pressure drop measurements (about 10 Pa), the tensile yield stress σ_t becomes insignificant when the gas velocity v_0 surpasses a gas velocity $v_1 < v_c$. Thus, there is a range of gas velocities, between v_1 and v_c, in which the measured yield stress of the fluidized bed stabilized by natural cohesive forces alone is practically negligible, albeit the bed possesses a solid structure as indicated by the nonvanishing value of the consolidation stress σ_c. The inset of Fig. 7 shows σ_t as a function of σ_c. As can be seen, σ_t is negligible for consolidation stresses below a critical value $\sigma_{c1}(v_1)$, which is $\sigma_{c1} \simeq 30$ Pa for the magnetite powder and $\sigma_{c1} \simeq 230$ Pa for the steel powder. Thus, the data indicate that an appreciably yield stress arises in these powders just because of the increase of consolidation above a threshold value. In particular, the tensile yield stress measured at marginal stability ($v_0 = v_c$, $\sigma_c = 0$) is below our experimental accuracy (± 10 Pa).

B.   Tensile yield stress of the magnetically stabilized bed

The measuring process described above has been performed in the presence of the magnetic field applied in the cross-flow configuration. In this way, the gas velocity at the transition to the stable state v_c, as well as the consolidation and tensile yield stresses have been measured. In Fig. 8 we show an example of fluidization-defluidization cycle for the steel powder bed in the presence of a magnetic field of strength $H = 2.8$ kA/m. The cycle in the absence of magnetic field is also plotted for comparison. As can be observed the gas velocity at marginal stability v_c is delayed from $v_c \simeq 1$ cm/s in the absence of field to $v_c \simeq 2$ cm/s in its presence. Note also that the tensile yield stress is notably increased. It can be also seen that the rate of increase of the gas pressure drop before the bed yields is decreased, which indicates that, in the presence of the magnetic field, particles rearrange in a configuration of higher porosity.

Data of the transition velocity v_c from the bubbling regime to the stable state are plotted in Fig. 9 as a function of the magnetic field strength. It is observed that the field effect becomes noticeable for strengths roughly above 2 kA/m for both powders. For $H \gtrsim 2$ kA/m, v_c increases steadily as the magnetic field strength is increased. Fig. 10 shows data on the measured values of the particle volume fraction at marginal stability ($\phi(v_c) = \phi_c$) as a function of the magnetic field strength. Generally, magnetic stabilization at higher fields occurs at higher gas velocities for higher expanded structures (smaller ϕ_c) although the decrease of ϕ is not pronounced. Remarkably, it is seen that the steel particles pack in structures of higher porosity (smaller ϕ) as compared to magnetite particles. Higher porosity packing is attributable to the aggregative nature of the finer particles [Valverde et al. 2004]. For fine particles, the ratio of interparticle attractive force to particle weight is larger, thus they tend to aggregate in porous structures.

Consolidation and tensile yield stress data as a function of the initial gas velocity $v_0 < v_c$ are shown in Fig. 11 for a magnetic field strength $H = 2.8$ kA/m. As can be seen, the presence of the magnetic field causes a slight increase of the consolidation stress since the bed is stabilized at higher gas velocities (see Fig. 8). On the other hand, the tensile yield stress is appreciable increased, specially for the steel powder. Remarkably, there persists a measurable σ_t up to the point of marginal stability ($v_c \simeq 2$ cm/s for steel and $v_c \simeq 1.2$ cm/s for magnetite), which can be only attributable to a magnetic cohesive stress since the

12

natural cohesive stress is negligible at these small consolidations (data from the naturally stabilized bed in the absence of magnetic field is shown for comparison).

The existence of a tensile yield stress at marginal stability in the MSB is clearly shown in Fig. 12, where pressure drop cycles are shown for steel and for initial gas velocities close to marginal stability ($H = 2.8$ kA/m, $v_0 \lesssim v_c \simeq 2$ cm/s). It is observed (Fig. 12 top) that just below marginal stability ($v_c \simeq 1.93$ cm/s) the pressure drop decreases abruptly as the gas velocity is decreased, which indicates the sudden appearance of a consolidation stress due to stabilization. The bottom figure shows a cycle from an initial gas velocity at marginal stability ($v_0 = 2$ cm/s) where this jump is not seen, thus $\sigma_c \simeq 0$. Yet there can be observed a pressure overshoot as the gas velocity is increased from v_0, which is indicative of the existence of a measurable yield stress even though the initial state was not consolidated. Magnetic stabilization seems thus to be determined by the development of a nonnegligible yield stress. This result contrasts with the conclusion inferred from Lee results [Lee 1983] obtained from the drawing-plate method, which suggested that the yield stress decreased abruptly to nearly zero at marginal stability [Rosensweig 1997].

Fig. 13 shows tensile yield stress data as a function of the strength of the magnetic field for the beds initialized at a fixed gas velocity ($v_0 = 0.51$ cm/s, $\phi_0 = 0.44$ for magnetite $\phi = 0.35$ for steel). Generally, for a given initial gas velocity v_0, the tensile yield stress of the stabilized bed stems from the contributions of the natural yield stress due to consolidation $\sigma_t(\sigma_c)$ (which we have measured in the absence of magnetic field, see Fig. 7 inset) and the yield stress purely induced by the magnetic field $\sigma_t(H)$

$$\sigma_t = \sigma_t(\sigma_c) + \sigma_t(H) \tag{2}$$

The first term in Eq. 2 takes into account that, at a given gas velocity $v_0 < v_c$, the stabilized bed in the presence of the magnetic field has a consolidation stress, which is larger than the naturally stabilized bed at v_0 (see Fig. 8). The inset of Fig. 13 shows the consolidation stress σ_c vs. the magnetic field strength for the beds magnetically stabilized at $v_0 = 0.51$ cm/s. Previous measurments of $\sigma_t(\sigma_c)$ (Fig. 7 (inset)) allows us to calculate the tensile strength just due to this consolidation stress, which is, for example, $\sigma_t \simeq 25$ Pa for steel and $\sigma_t \simeq 15$ Pa for magnetite at $H = 5$ kA/m. Data from Fig. 13 shows therefore that the contribution from consolidation is a minor contribution to the total tensile yield stress as compared to the purely magnetic stress $\sigma_t(H)$. Moreover, this contribution becomes smaller

13

as marginal stability is approached, where σ_c becomes smaller and the natural yield stress is negligible.

IV.   DISCUSSION

A.   Tensile yield stress of the naturally stabilized bed

In the absence of external magnetic field, the main interparticle attractive force between unloaded particles is just the natural van der Waals attractive force [Castellanos 2005], which is produced by the interaction of fluctuating molecular electric dipole fields. Assuming that retardation effects are negligible and that the interaction between molecules is pairwise, Hamaker [Hamaker 1937] summed up all the interactions between two spherical and rigid particles at contact with diameters d_1 and d_2 and arrived at the approximate expression for the attractive force

$$f_{vdW} \simeq \frac{A d^*}{12 z_0^2}, \tag{3}$$

where A is the Hamaker constant, $d^* = d_1 d_2/(d_1 + d_2)$ is the reduced diameter, and $z_0 \simeq 3-4$ Å is the distance of closest approach between two molecules. Because of the short range of the molecular interaction, the van der Waals force is actually determined by the local radius of curvature of the surface asperities at contact. Therefore the typical size of the surface asperities d_a must be used in Eq. 3 instead of the particle diameters. A typical value reported for the size of surface asperities of fine powder particles is $d_a \simeq 0.2\mu$m [Rietema 1991], while a typical value of A is $A \simeq 10^{-19}$J [Visser 1972, Ross and Morrison 1988]. Thus we can estimate an attractive force $f \simeq f_{vdW} \simeq 10$ nN between our experimental particles. The tensile yield stress of the powder that arises from the existence of this interparticle attractive force can be estimated by means of the Rumpf averaging equation [Rumpf 1958, Quintanilla et al. 2001b] as

$$\sigma_t \sim f_{vdW} \frac{\zeta \, \phi}{\pi d_p{}^2} \tag{4}$$

where ζ is the coordination number (average number of contacts per particle) that can be related to the particle volume fraction ϕ by the equation $\zeta \simeq (\pi/2)(1 - \phi)^{-3/2}$ (ref. [Suzuki et al. 1981]). Using as typical values $f = f_{vdW} = 10$ nN, $d_p = 35\mu$m, and $\phi = 0.4$,

it is estimated $\sigma_t \simeq 4$ Pa, which is below our experimental indeterminacy (± 10 Pa). It is therefore explainable that the measured tensile yield stress of the fluidized bed, stabilized by the attractive van der Waals forces alone, is negligible at marginal stability ($\sigma_c = 0$).

As the gas velocity is decreased below the point at marginal stability, the powder is consolidated ($\sigma_c > 0$), which may induce plastic deformation at interparticle contacts. Equation 3 cannot explain however the enhancement of interparticle attractive force due to plastic deformation of interparticle contacts due to consolidation stresses, which gives an appreciable yield stress for consolidation stresses above $\sigma_c \simeq 30$ Pa, in the case of magnetite, and $\sigma_c \simeq 230$ Pa, in the case of steel. The critical load on the contact for the initiation of plastic yield within the bulk of the particle depends on mechanical material properties such as yield strength in compression and Young modulus. Plastic yielding is considered in more elaborated theories, such as the Mesarovic and Johnson theory (see [Castellanos 2005] for a detailed review). The analysis of plastic deformation is beyond the scope of this paper, which is focused on the effect of the magnetic field on the tensile yield stress. Our measurements of the tensile yield stress in the absence of magnetic field will serve us to extract the yield stress due to consolidation from the total yield stress measured in the presence of a magnetic field. This will serve to obtain the contribution to the yield stress just due to the magnetic field.

B. Extension of the stable fluidization regime

The extension of the stable fluidization interval to higher gas velocities in the presence of the magnetic field (Fig. 9) can be attributed to the increase of the interparticle attractive force due to the magnetization of the particles. A rigorous calculation of the force between magnetized particles would require a large number of multipolar moments when the particles are in contact [Tan and Jones 1993]. Nevertheless, in the range of field strengths applied, the dipolar approximation can be used for an estimation of order of magnitude of the contact force [Tan and Jones 1993]. The attractive force between two aligned dipoles of moment m_p separated by a distance d_p is given by [Taylor et al. 2008]

$$f_m = \frac{3\mu_0 m_p^2}{2\pi d_p^4} \tag{5}$$

15

where μ_0 is the permeability of free space ($4\pi \times 10^{-7}$ H/m). According to our rheological measurements, in the presence of an external field, the magnetic particles would be magnetized with a dipolar moment $m_p = \chi_p H (1/6)\pi d_p^3$. The effect of the magnetic field on extending the stable fluidization interval becomes noticeable at $H \simeq 2$ kA/m. From Eq. 5 it can be estimated that the magnetic force becomes at $H \simeq 2$ kA/m a few times the van der Waals force. For smaller fields, the magnetic force is comparable or smaller than the van der Waals force and consequently there is not a notable effect of the magnetic field on the transition to stability. Thus, the data suggests that the transition to the stable state in the presence of the magnetic field is ruled by the strength of the magnetic attractive force between the particles.

C. Tensile yield stress of the magnetically stabilized bed

The yield stress σ_y of a MSB is attributable to the strength of the attractive force at the contacts between the particles and their arrangement in the bed. It should depend on particle magnetization $M_p = \chi_p H_0$ and particle volume fraction ϕ. A simple dimensional analysis leads to the equation [Rosensweig 1997]

$$\sigma_y = \mu_0 f(\phi)\chi_p^2 H_0^2 \tag{6}$$

Rosensweig [Rosensweig 1997] obtained $f(\phi) = A/(1-\phi)^\alpha$, where $A = 3.3\times10^{-5}$ and $\alpha = 12$, by fitting Eq. 6 to Lee results [Lee 1983] on iron particles in the range $0.41 < \phi < 0.52$ [Rosensweig 1997]. It must be remarked however that the uncertainty found in the fitting parameters was great. For example, the constant A decreased to $A = 0.5 \times 10^{-5}$ when an alternating field (60 Hz) was applied to magnetize the bed.

By using a point dipole approximation, the magnetic cohesive stress of three-dimensional arrays of linearly magnetizable particles was obtained [Jones 1995] as $\sigma_s = (3/4\pi)\mu_0\chi^2\alpha H_\perp^2$ where $H_\perp$ is the strength of the normal component of the field to the plane surface. The parameter α is strongly dependent upon the assumed packing. For example, $\alpha = 1.83$ in a cubic array and is much smaller in a hexagonal close-packed array. The yield stress on a plane parallel to the magnetic field is theoretically expected to be negative although no experimental evidence for negative cohesion has been reported in beds of magnetizable particles [Jones et al. 1987]. Modeling the magnetized particles as point dipoles oriented

along the field direction is however too simplistic. This is shown in Fig. 14, where the lines of magnetic flux density field numerically calculated by FEM are shown in a packed bed of magnetic beads ($\chi_p = 5.33$) subjected to an externally applied horizontal magnetic field. As can be seen the field is guided across the magnetic beads like in a magnetic circuit and penetrates almost perpendicularly through the particle contacts, which gives a net cohesive force between the particles. Interparticle contacts can be thus stable in the cross-flow field configuration while the point dipole approximation would predict a repulsive force in the horizontal plane. In practice the yield stress would be obtained as an average of interparticle cohesive forces, which is expected to be affected by the structuring of particles during fluidization and transition to stable fluidization. The field distribution at interparticle contacts yields north-to-south poles attractive force $F \propto M_p^2$. Thus, it is expected that the yield stress is proportional to H_0^2 as obtained from the dimensional analysis.

The dashed curves in Fig. 13 are the best fits of Eqn. 6 to the experimental data on the tensile yield stress, where $f(\phi) = 2.18(1 - \phi)^{5.84}$ for both powders. In contrast with Lee results [Lee 1983] on iron beads, we find that the yield stress increases as the particle volume fraction ϕ is decreased. A reasonable explanation to this discrepancy is that, in our case, ϕ is closely related to the influence of the field on particle arrangement. In the fluidized state, particles are free to move and, being magnetized by the external field, are prone to form chains that strengthen the bed when the gas velocity is decreased. Particle chaining should be however influenced by the aggregative nature of the particles in the absence of applied field as seen for the steel powder. The dipolar interaction is expected to be enhanced between aggregates [Lalatonne et al. 2004] of our steel fine particles as compared to the interaction between our mostly individual magnetite particles and the nonaggregated iron beads used by Lee [Lee 1983].

V. VISUALIZATION OF PARTICLE CHAINS

Yield stress data indicates a role of the magnetic field on particle organization during magnetofluidization possibly consisting of the development of particle chains through inter-particle magnetic interaction. To further investigate this effect we made direct observations of particle arrangement in the fluidized bed as affected by the presence of a magnetic field. A piece of adhesive tape was carefully lowered edgewise into the fluidized bed so as to

cleave it perpendicular to the gas flow path. Then, on carefully withdrawing the card, the layer of powder adhered to the tape was observed at the optical microscope. Images were preferentially taken from the vicinity to the free surface, where the concentration of particles adhering to the tape is not large, allowing us to discriminate for a possible particle structuring.

Examples of pictures obtained in the absence of applied magnetic field are shown in Fig. 15. Visual inspection shows that steel particles in fluidization are naturally more aggregated as it was inferred from SEM images (Fig. 1). Examples of pictures obtained in the presence of applied magnetic field are shown in Fig. 16. As it was suggested by yield stress measurements these pictures show that, in the presence of the magnetizing field, the arrangement of the particles is severely affected. Magnetite particles are seen to form quasilineal aggregates composed of a few particles due to the magnetic attraction forces between the otherwise nonaggregated particles. The morphology of these aggregates could be expected since magnetite particles were mostly found individually in the absence of field. In contrast, we observe for the steel magnetized bed relatively larger aggregated structures, whose formation is attributable to the enhanced interaction between the already existing aggregates in the absence of field. These results suggest that, in spite of having similar bulk magnetization, the aggregative nature of the steel powder in the absence of field favors structuring in the fluidized bed when a magnetic field is applied. An analogous coupling between natural aggregation and dipolar interaction has been recently reported for magnetic nanoparticles dispersed in solution, where only clustered nanocrystals due to enhance van der Waals force exhibit chain-like structures when the field is applied [Lalatonne et al. 2004].

Observations reported in this work might be of interest to geological studies. Measuring the anisotropy of magnetic susceptibility (AMS) due to flow alignment of magnetic particles is a method routinely used by geologists to identify palaeoflow directions in volcanic rocks and sediments [Potter and Stephenson 1988]. In the presence of a magnetic field, the sedimentary magnetic anisotropy should be influenced by the effect of the magnetic field on the process of sedimentation. In spite of its unquestionable role, it is commonly accepted that this effect has been overlooked, which possibly leads to erroneous interpretation of data on magnetic anisotropy [Shashkanov and Kosterov 1994]. Our results suggest that natural aggregation of magnetic particles should be a parameter to be considered since it could influence their flow arrangement if a magnetic field is present.

VI.   CONCLUSIONS

In conclusion, we have investigated in this work the yield stress of fluidized beds of fine magnetic particles stabilized by van der Waals and magnetic forces. The tensile yield stress at marginal stability in the absence of externally applied field is found to be negligible ($\sigma_t \lesssim 10$ Pa). By imposing a cross-flow magnetic field to the fluidized bed, the interval of stable fluidization is extended to higher gas velocities for fields of strength $H \gtrsim 2$ kA/m, which give rise to an interparticle magnetic force that prevails against the natural van der Waals force. It has been shown that the high permeability of the particles gives rise to north-to-south poles attractive force at interparticle contacts independently of the orientation of the externally applied magnetic field, which explains why the bed can be stabilized by a horizontal field against the expected result from the point-dipole approximation. As the strength of the field is increased the gas velocity at marginal stability is increased. The yield stress of the magnetostabilized bed (MSB) is appreciably at marginal stability even though the bed is jammed in a state of zero consolidation and scales with the square of the field strength. According to visual observations the aggregative nature of the powders in the absence of field favors the formation of large scaled branched structures in the MSB, which enhances the yield stress. In contrast, if particles in the naturally fluidized bed behave individually, structures in the MSB just consist of quasilineal particle chains, which give rise to a modest increase of the yield stress. Thus our work shows that the behavior of the MSB is correlated to the natural behavior of the bed in the absence of applied field.

VII.   ACKNOWLEDGEMENTS

[Albert 1985] Albert R. V. and C. Tien. Particle collection in magnetically stabilized fluidized filters. AIChE J. 31, 288–295 (1985).

[Bauccio 1994] http://www.matweb.com. Source: ASM Engineered Materials Reference Book, Second Edition, Michael Bauccio, Ed. ASM International, Materials Park, OH, 1994.

[Carman 1937] Carman P. C. Fluid flow through granular beds. Trans. Inst. Chem. Engrs. 15, 150–166 (1937).

[Castellanos et al. 2004] Castellanos A., Valverde J.M. and M.A.S. Quintanilla. The Sevilla Powder Tester: A tool for characterizing and investigating the physical properties of fine cohesive powders. KONA Powder and Particle 22, 66–81 (2004).

[Castellanos 2005] Castellanos A. The relationship between attractive interparticle forces and bulk behaviour in dry and uncharged fine powders. Adv. Phys. 54, 263–376 (2005).

[Cohen and Tien 1991] Cohen A. H. and C. Tien. Aerosol filtration in a magnetically stabilized fluidized bed. Powder Technol. 64, 147-158 (1991).

[Constantineaua et al. 2007] Constantineaua J.P., Grace J.R., Lima C.J. and G.G. Richards. Generalized bubbling-slugging fluidized bed reactor model. Chem. Eng. Sci. 62, 70–81 (2007).

[Geldart 1973] Geldart D. Types of gas fluidization. Powder Technol. 7, 285–293 (1973).

[Hamaker 1937] Hamaker H. C. The London-Van der Waals attraction between spherical particles. Physica 4, 1058–1072 (1937).

[Hristov 1996] Hristov J. Y. Fluidization of ferromagnetic particles in a magnetic field .1. The effect of field line orientation on bed stability. Powder Technol. 87, 59–66 (1996).

[Hunt et al. 1995] Hunt C. P., Moskowitz B. M. and S. K. Banerjee. Magnetic Properties of Rocks and Minerals, in *Rocks Physics and Phase Relations: A Handbook of Physical Constants*. Edited by T. J. Ahrens (American Geophysical Union Books Board, USA, 1995) 189-204.

[Jackson 2001] Jackson R. The dynamics of fluidized particles, Cambridge University Press, Cambridge, 2000.

[Johnson and Melcher] Johnson T. W. and J. R. Melcher. Electromechanics of electrofluidized beds. Ind. Eng. Chem. Fundam. 14, 146–153 (1975).

[Jones 1995] Jones T. B. Electromechanics of particles, Cambridge University Press, Cambridge, 1995.

[Jones et al. 1987] Jones T. B., Whittaker G. L. and T. J. Sulenski. Mechanics of magnetic powders. Powder Technol. 49, 149–164 (1987).

[Karkkainen et al. 2001] Karkkainen K., Sihvola A. and K. Nikoskinen. Analysis of a Three-Dimensional Dielectric Mixture with Finite Difference Method. IEEE Trans. Geosci. Remote Sensing. 39, 1013–1018 (2001).

[Lalatonne et al. 2004] Lalatonne Y., Richardi J. and M. P. Pileni. Van der Waals versus dipolar

forces controlling mesoscopic organizations of magnetic nanocrystals. Nature Mat. 3 121-125 (2004).

[Lee 1983] Lee W. K. The rheology of magnetically stabilized fluidized solids. AIChE Symp. Ser. 79, 87–96 (1983).

[Lee 1991] Lee W. K. A review of the rheology of magnetically stabilized fluidized beds. Powder Technol. 64, 69–80 (1991).

[Melcher 1977] Melcher J R. Overview of electrostatic devices for control of submicrometer particles. Proceed. of the IEEE 65, 1659–1672 (1977).

[Mills 2004] Mills A. A. The Lodestone: History, Physics, and Formation. Annals of Science. 61, 273319 (2004).

[Potter and Stephenson 1988] Potter D. K. and A. Stephenson. Single domain particles in rocks and magnetic fabric analysis. Geophys. Res. Lett. 15, 1097-1100 (1988) .

[Quintanilla et al. 2001] Quintanilla M. A. S., Valverde J. M., Castellanos A. and R. E. Viturro. Phys. Rev. Lett. 87, 194301 (2001).

[Quintanilla et al. 2001b] Quintanilla M. A. S., Castellanos A. and J. M. Valverde. Correlation between bulk stresses and interparticle contact forces in fine powders. Phys. Rev. E 64, 031301 (2001) .

[Quintanilla et al. 2004] Quintanilla M. A. S., Castellanos A. and J. M. Valverde. Granular avalanches: Deterministic, correlated and decorrelated dynamics. Europhys. Lett. 68 818-824 (2004) .

[Quintanilla et al. 2006] Quintanilla M.A.S., Valverde J.M. and A. Castellanos. The transitional behavior of avalanches in cohesive granular materials. J. Stat. Mech. P07015, 1-26 (2006).

[Rhodes et al. 2005] Rhodes M. J., Wang X. S., Forsyth A. J., Gan K. S. and S. Phadtajaphan. Use of a magnetic fluidized bed in studying Geldart Group B to A transition, Chem. Eng. Sci. 56, 5429-5436 (2001) .

[Rietema 1991] Rietema K. The Dynamics of Fine Powders, Elsevier, London, 1991.

[Rosensweig 1979] Rosensweig R. E. Fluidization: Hydrodynamic stabilization with a magnetic field. Science 204, 57–60 (1979).

[Rosensweig 1979b] Rosensweig R. E. Magnetic stabilization of the state of uniform fluidization. Ind. Eng. Chem. Fundam. 18, 260–269 (1979).

[Rosensweig 1997] Rosensweig R. E. Ferrohydrodynamics, Dover publications, New York, 1997.

[Ross and Morrison 1988] Ross S. and I.D. Morrison. Colloidal Systems and Interfaces, Willey-Interscience, New York, 1988.

[Rumpf 1958] Rumpf H. Grundlagen and methoden des granulierens. Chemie Ing. Techn. 30, 144–158 (1958) .

[Seville and Clift 1984] Seville J.P.K. and R.C. Clift. The effect of thin liquid layers on fluidization characteristics. Powder Technol. 37, 117–129 (1984).

[Shashkanov and Kosterov 1994] Shashkanov V. A. and A. A. Kosterov. Dependence of magnetic anisotropy of sedimentary rocks on sedimentation field. Physics of the Solid Earth 30, 82-87 (1994) .

[Siegell 1984] Siegell J. H. and C. A. Coulaloglou. Magnetically stabilized fluidized beds with continuous solids throughput. Powder Technol. 39, 215–222 (1984).

[Siegell 1988] Siegell J. H. Magnetically frozen beds. Powder Technology 55, 127–132 (1988) .

[Siegell 1989] Siegell J. H. Early Studies of magnetized-fluidized beds. Powder Technol. 57, 213–220 (1989).

[Sundaresan 2003] Sundaresan S. Instabilities in fluidized bed. Annu. Rev. Fluid Mech. 35, 63–88 (2003).

[Suzuki et al. 1981] Suzuki M., Makino K., Yamada M. and K. Iinoya. Study on the coordination number in a system of randomly packed, uniform-sized spherical particles. Int. Chem. Engng. 21, 482–488 (1981).

[Tan and Jones 1993] Tan C. and T. B. Jones. Interparticle force measurements on ferromagnetic steel balls. J. Appl. Phys. 73, 3593–3598 (1993).

[Taylor et al. 2008] Taylor K., King P. J. and M. R. Swift. Influence of magnetic cohesion on the stability of granular slopes. Phys. Rev. E 78, 031304 (2008).

[Valverde et al. 1998] Valverde J. M., Ramos A., Castellanos A. and P. K. Watson, The tensile strength of cohesive powders and its relationship to consolidation, free volume and cohesivity. Powder Tech. 97, 237–245 (1998).

[Valverde et al. 2001] Valverde J. M., Castellanos A. and M. A. S. Quintanilla. Effect of vibration on the stability of a gas-fluidized bed of fine powder. Phys. Rev. E 64, 021302 (2001).

[Valverde et al. 2000] Valverde J. M., Castellanos A., Ramos A., Perez A. T., Morgan M. A. and P. K. Watson. An automated apparatus for measuring the tensile strength and compressibility of fine cohesive powders. Rev. Sci. Instrum. 71, 2791–2795 (2000).

[Valverde et al. 2001] Valverde J. M., Castellanos A. and M.A.S. Quintanilla. Self-diffusion in a gas-fluidized bed of fine powder. Phys. Rev. Lett. 86, 3020–3023 (2001) .

[Valverde et al. 2003] Valverde J. M., Castellanos A. and M. A. S. Quintanilla. The memory of granular materials. Contemp. Phys. 44, 389–399 (2003).

[Valverde et al. 2004] Valverde J.M., Castellanos A. and M.A.S. Quintanilla. Jamming threshold of dry fine powders. Phys. Rev. Lett. 92, 258303 (2004).

[Valverde et al. 2009] Valverde J. M., Espin M. J., Quintanilla M. A. S. and A. Castellanos. Magnetofluidization of fine magnetite powder. Phys. Rev. E 79, 031306 (2009).

[Visser 1972] Visser J. On Hamaker constants: a comparison between Hamaker constants and Lifshltz - van der Waals constants. Advan. Colloid Interface Sci. 3, 331–363 (1972).

[Xie and Geldart 1995] Xie H.-Y. and D. Geldart. Fluidization of FCC powders in the bubble-free regime: effect types of gases and temperature. Powder Technol. 82, 269–277 (1995).
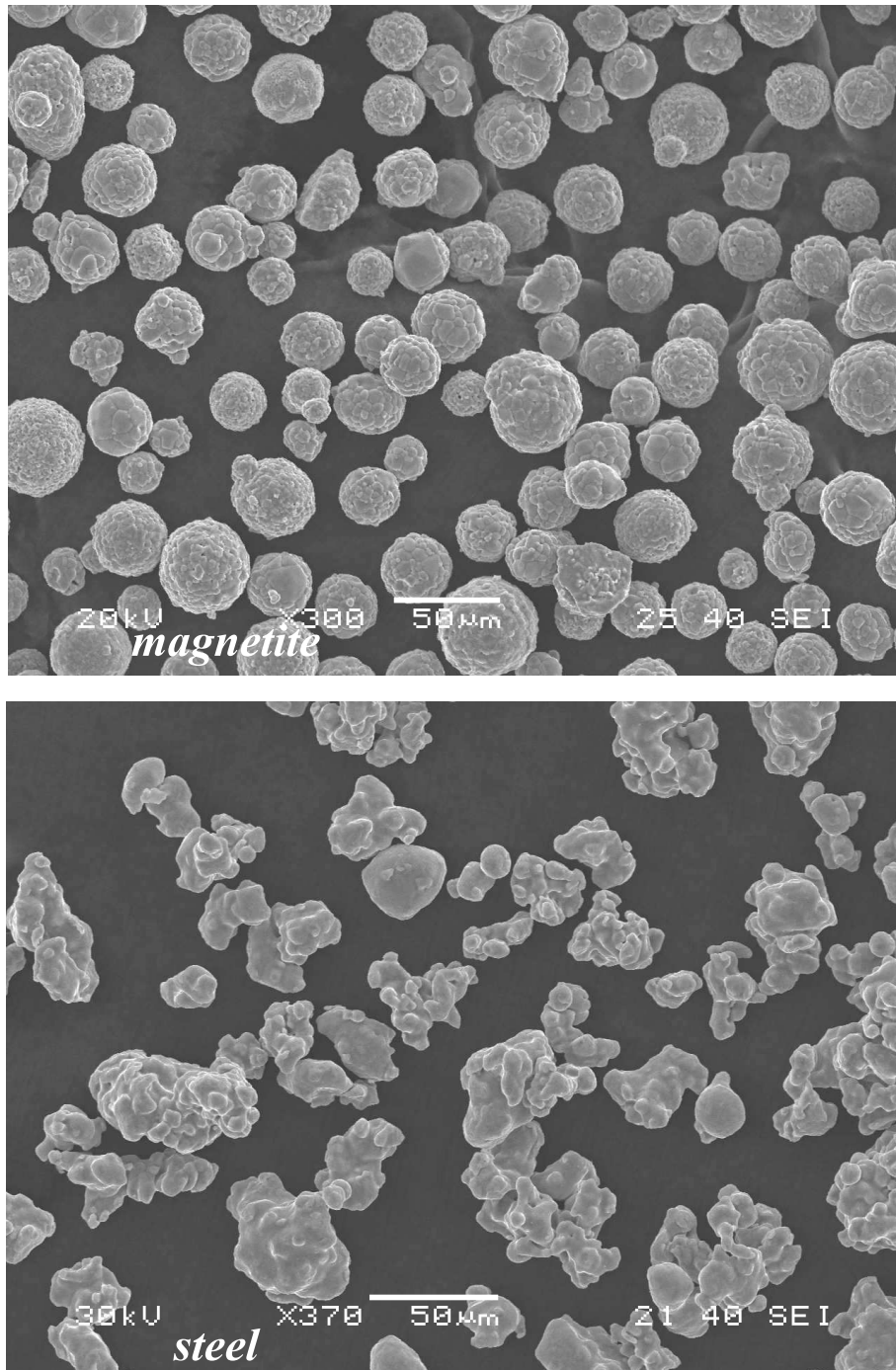
FIG. 1: SEM photographs of the steel and magnetite particles used in the magnetofluidization experiments reported in this paper.
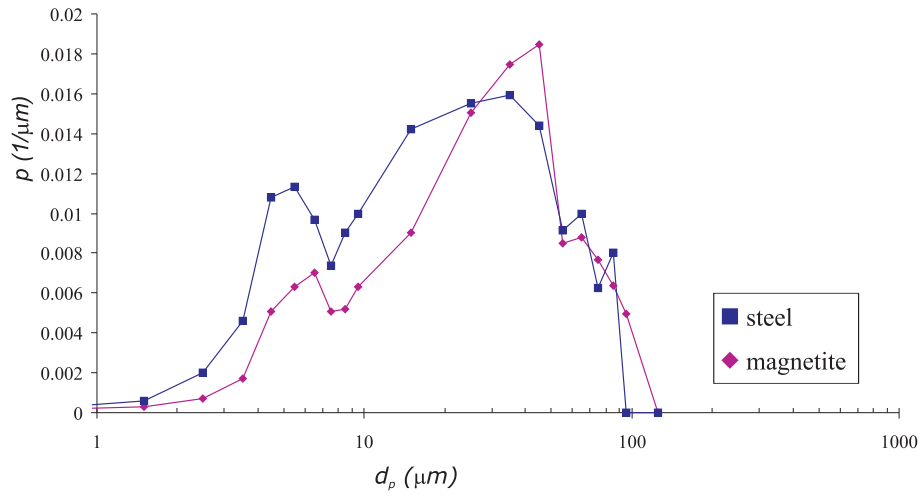
FIG. 2: Normalized particle size distributions of the powders used in this work.
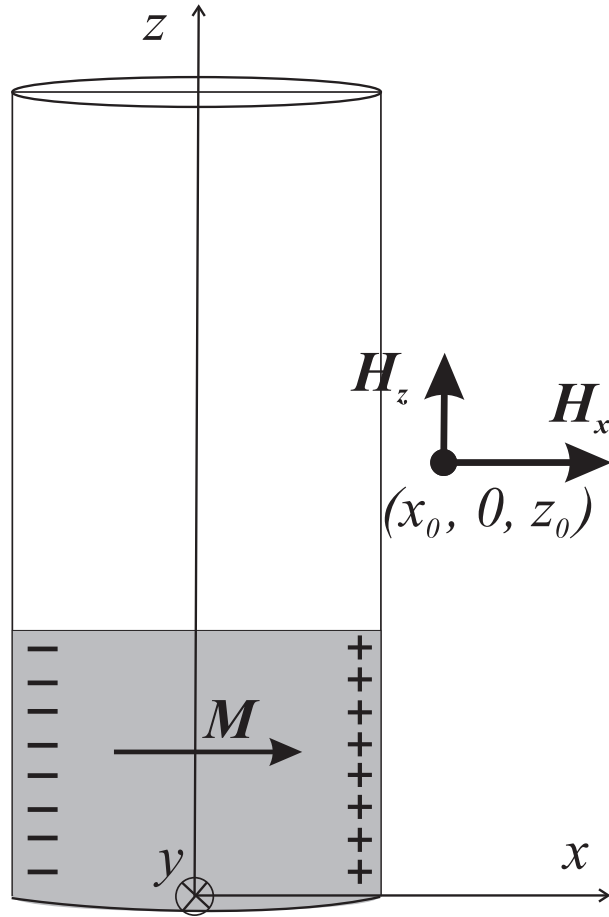
FIG. 3: Sketch of the 2.54 cm dia. powder bed magnetized by an external field applied in the x direction. The external field magnetizes the powder with a magnetization $\mathbf{M}$ in the x direction. The x component of the total magnetic field H_x is measured by the probe at the point $x_0 = 2.51$ cm, $y_0 = 0$, $z_0 = 2.4$ cm. The settled bed height is $h = 1.9$ cm.
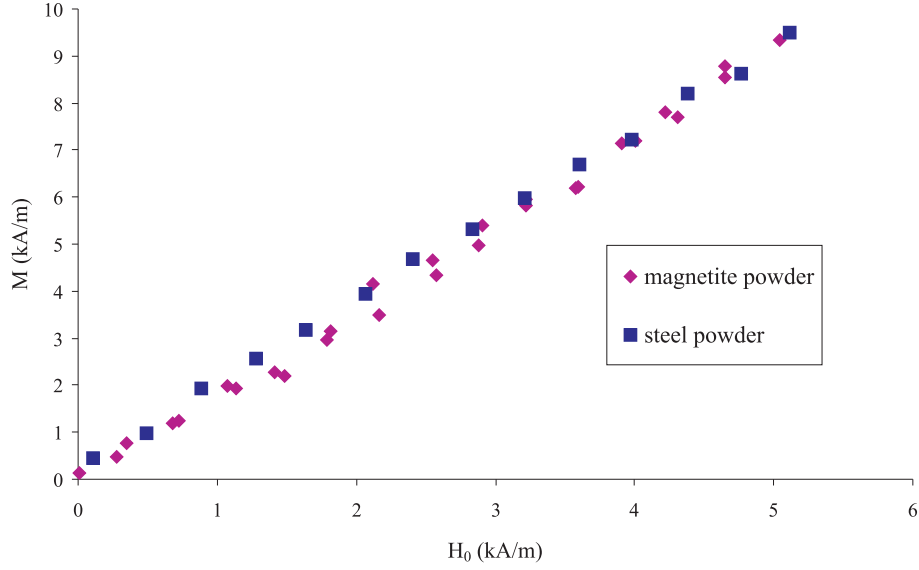
FIG. 4: Bulk magnetization of the powders used in the experiments as a function of the strength of the external field applied.
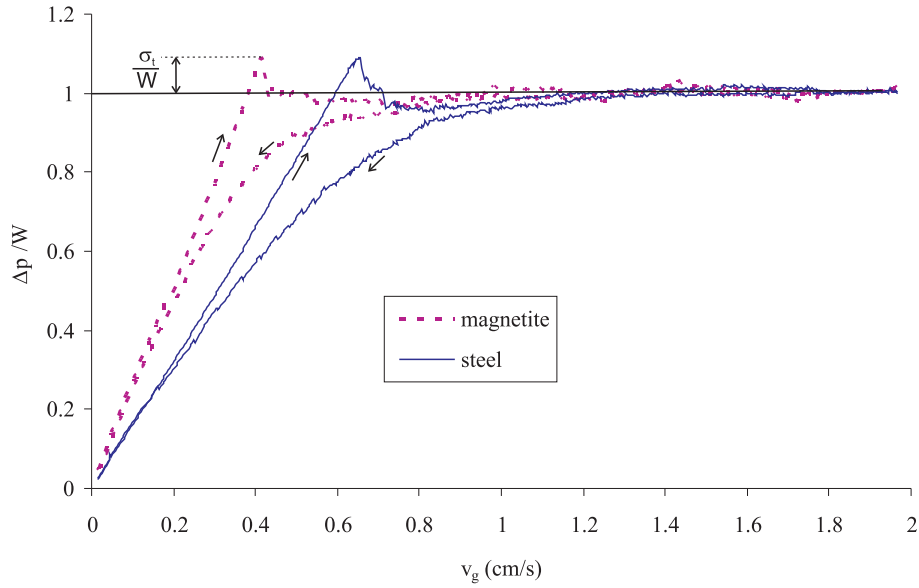
FIG. 5: Gas pressure drop across the powder beds as a function of superficial gas velocity during the fluidization-defluidization cycles in the absence of externally imposed magnetic field (H off). Examples of two cycles are plotted corresponding to the magnetite and steel powder beds settled under its own weight ($v_0 = 0$ cm/s). The gas pressure drop is made nondimensional with the powder weight per unit area ($W = 774$ Pa for steel and $W = 511$ Pa for magnetite). Pressure overshoot that gives the tensile strength σ_t is indicated for magnetite.
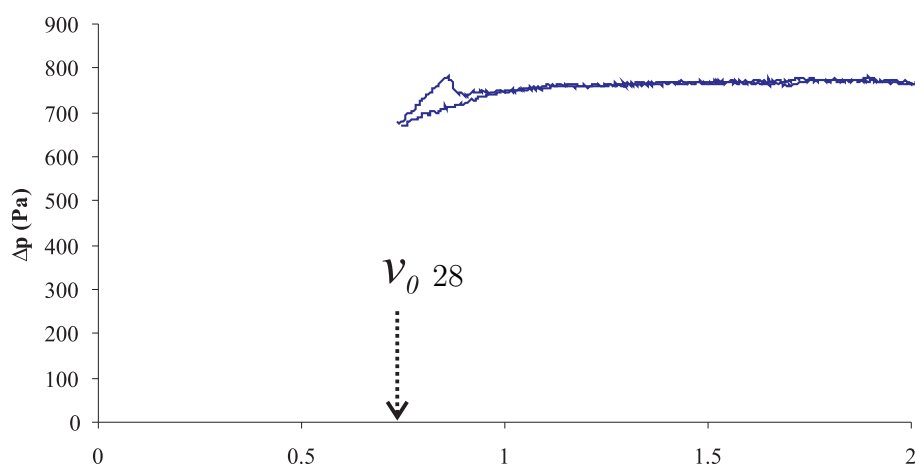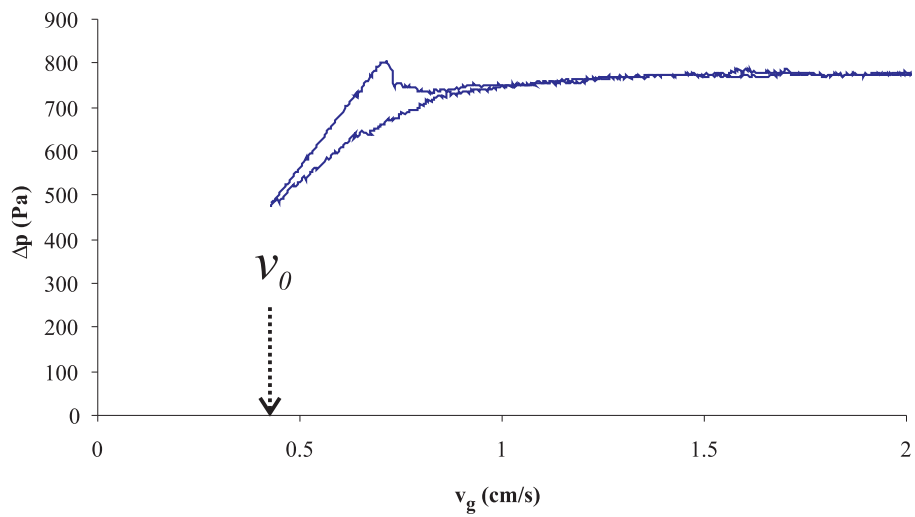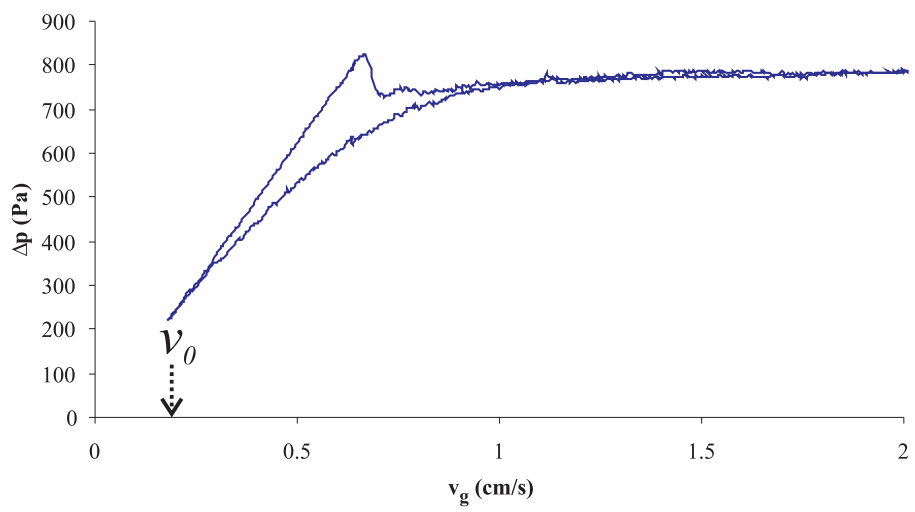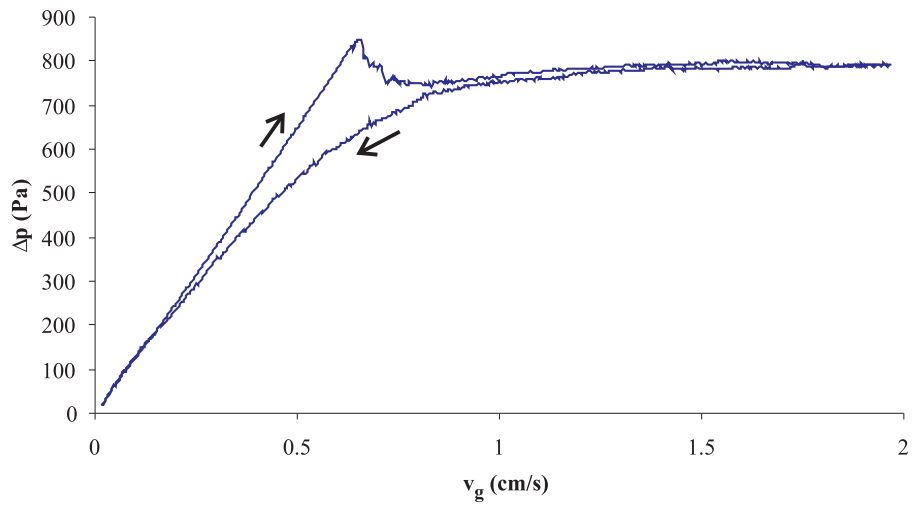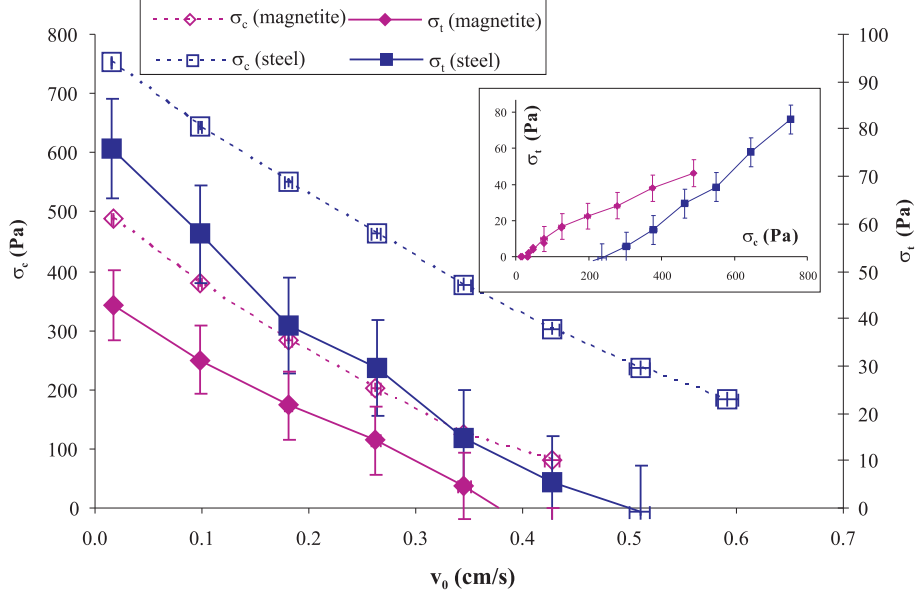
FIG. 7: Consolidation stress (left axis) and tensile yield stress (right axis) of the powder bed as a function of the initial gas velocity v_0. The inset show the tensile yield stress as a function of the consolidation stress.
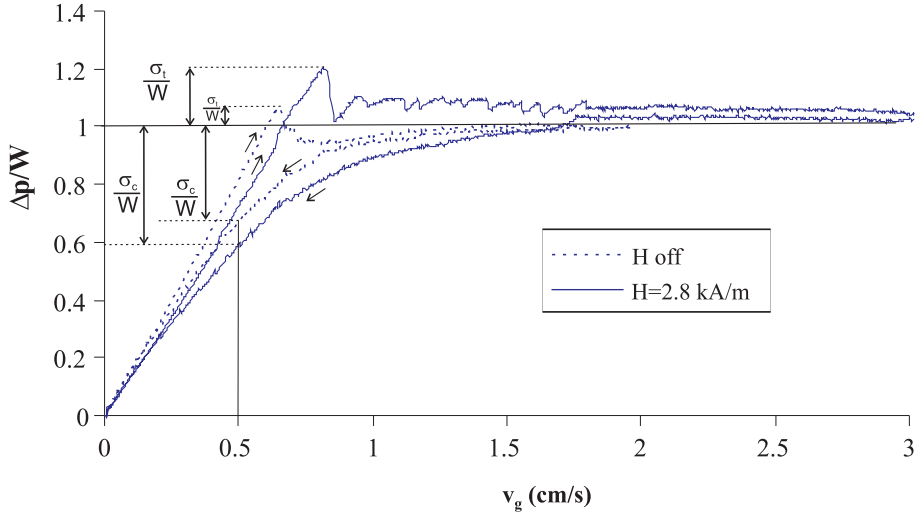
FIG. 8: Fluidization-defluidization cycles of the steel powder bed in the absence of an externally applied magnetic field (H off) and in the presence of a magnetic field of strength $H = 2.8$ kA/m. The pressure drop Δp is made nondimensional with the weight per unit area ($W = 774 Pa$). The tensile strength σ_t for $v_0 = 0$cm/s is indicated in the absence and presence of magnetic field. The consolidation stress σ_c when the gas flow is decreased to $v_0 = 0.5$ cm/s is indicated in the absence and presence of magnetic field.
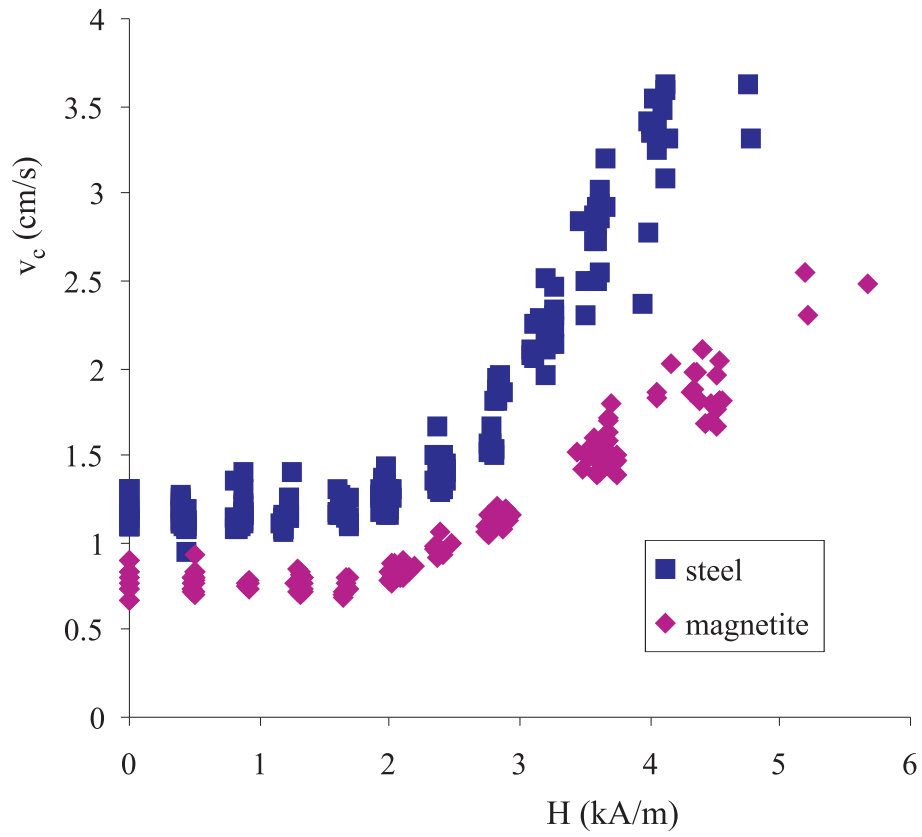
FIG. 9: Gas velocity at the transition to the stable fluidization regime v_c as a function of the magnetic field strength for the fluidized steel and magnetite powder beds.
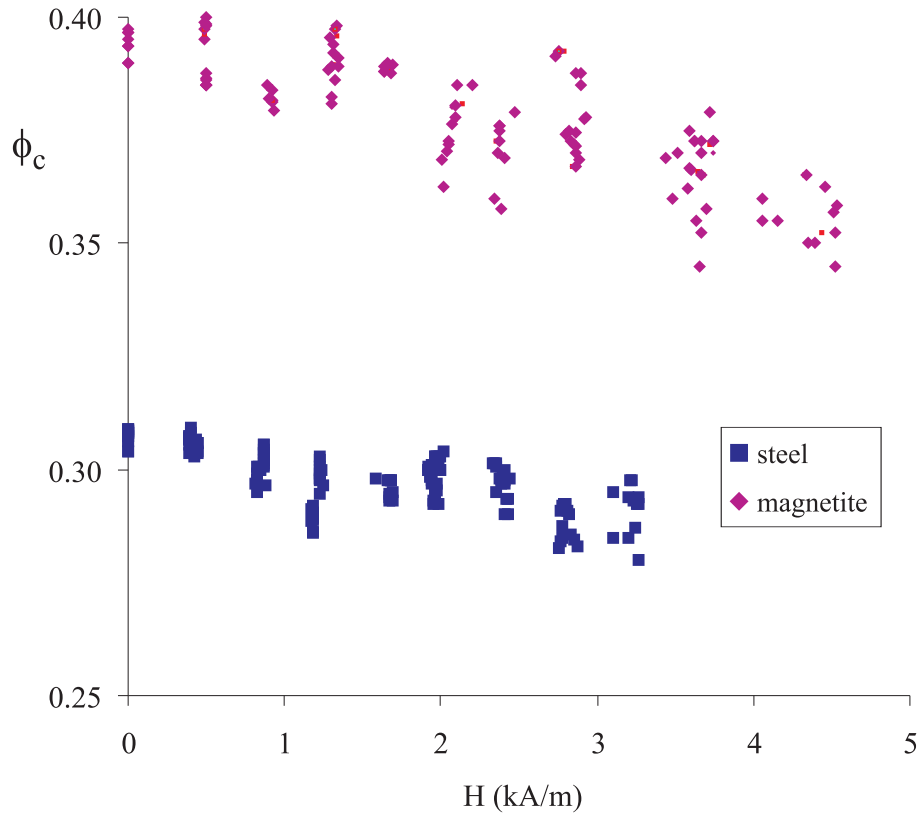
FIG. 10: Particle volume fraction ϕ of the fluidized bed at marginal stability (gas velocity $v_g = v_c$) as a function of the strength of the magnetic field for the fluidized steel and magnetite powder beds.
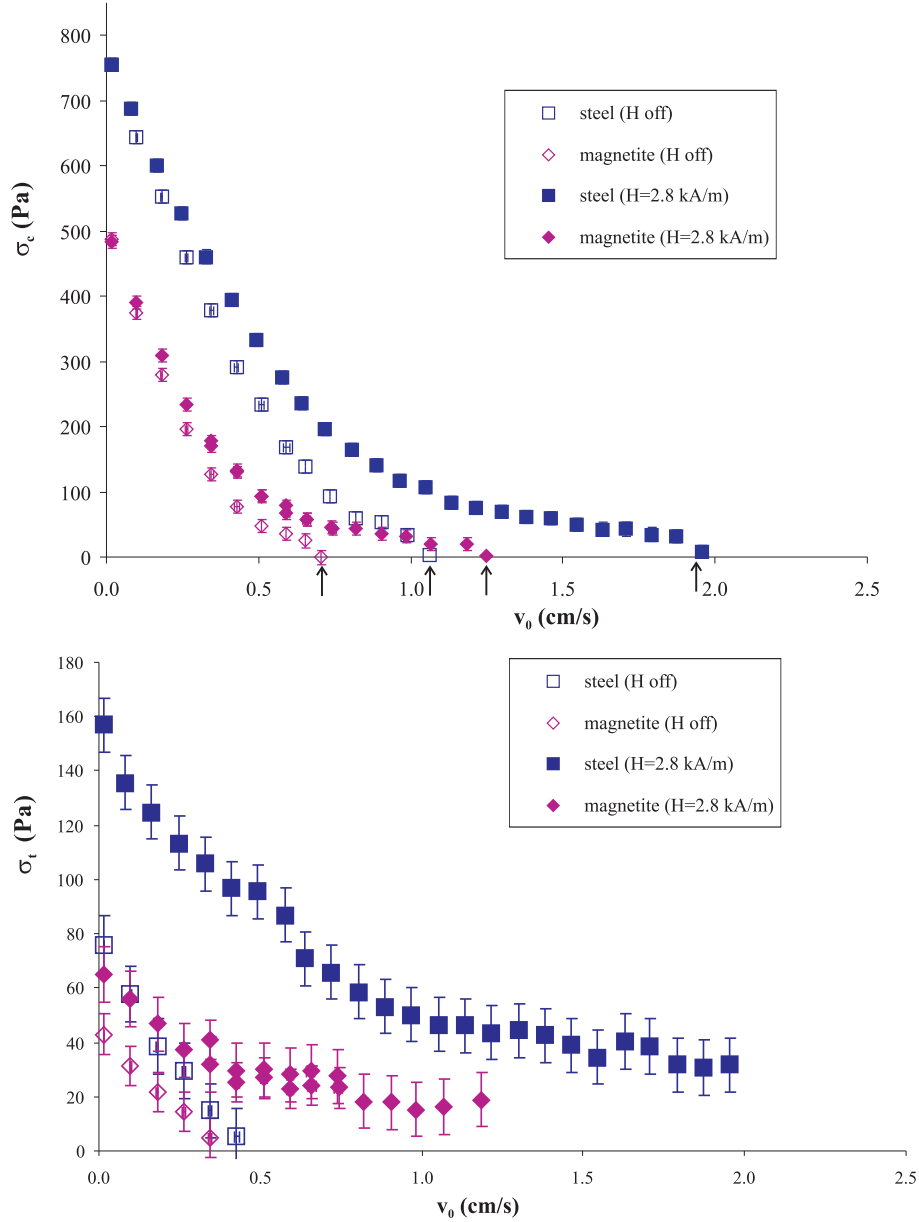
FIG. 11: Consolidation stress (top) and tensile yield stress (bottom) of the steel and magnetite fluidized beds as a function of the initial gas velocity v_0. Data are shown for experiments performed in the presence of a magnetic field of strength 2.8 kA/m and in the absence of magnetic field for comparison. The arrows in the top figure indicate the gas velocities v_c at marginal stability.
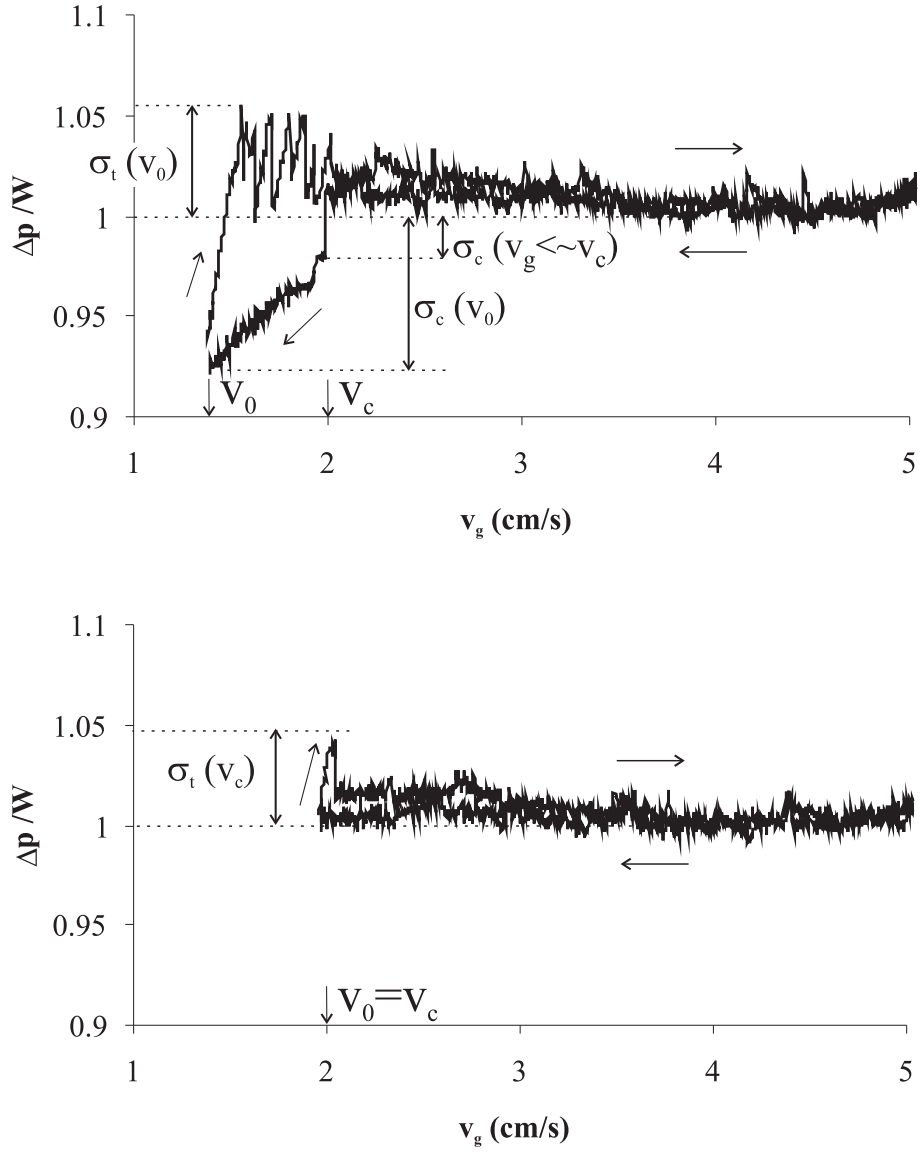
FIG. 12: Fluidization-defluidization cycles of the steel powder bed in the presence of a magnetic field of strength $H = 2.8$ kA/m from initial gas velocities v_0 close to marginal stability ($v_c \simeq 2$ cm/s). Top: $v_0 = 1.4$ cm/s. Bottom: $v_0 = v_c$.
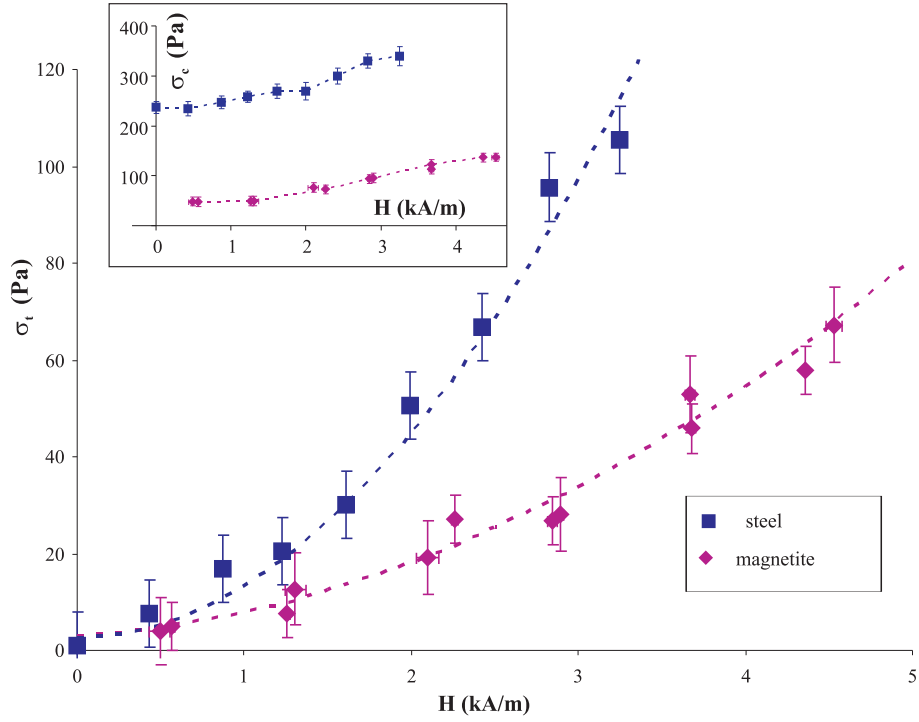
FIG. 13: Tensile yield stress of the steel and magnetite powder beds as a function of the strength of the magnetic field for an initial gas velocity $v_0 = 0.51$ cm/s. The dashed lines represent the fitting of Eq. 6 to the data. The inset shows the consolidation stress as a function of the strength of the magnetic field ($v_0 = 0.51$ cm/s).
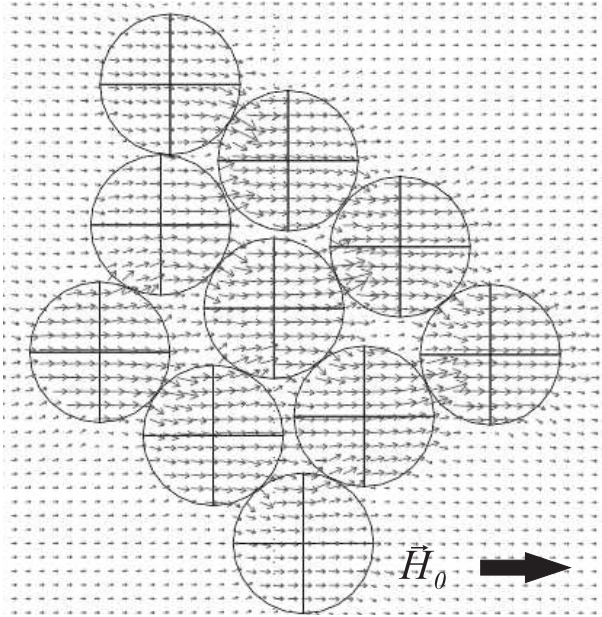
FIG. 14: Magnetic flux density lines obtained by FEM for packed bed of spherical beads ($\chi_p = 5.33$). The externally applied field H_0 is horizontal.
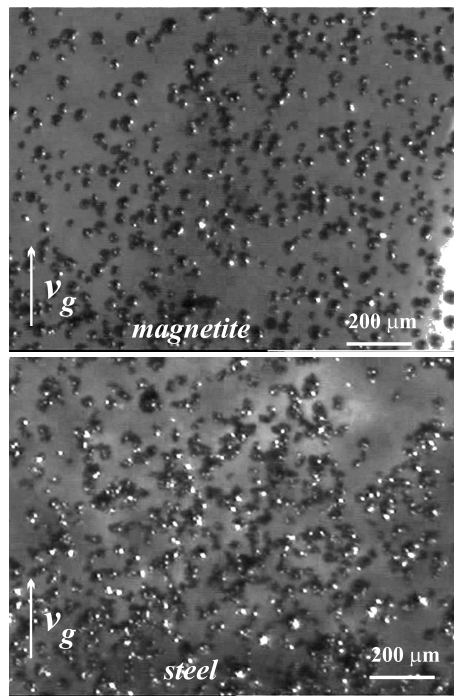

FIG. 15: Optical microscope images of the steel and magnetite particles taken from the fluidized bed in the absence of magnetic field applied at gas velocities $v_g = 2$ cm/s (magnetite) and $v_g = 2.6$ cm/s (steel).
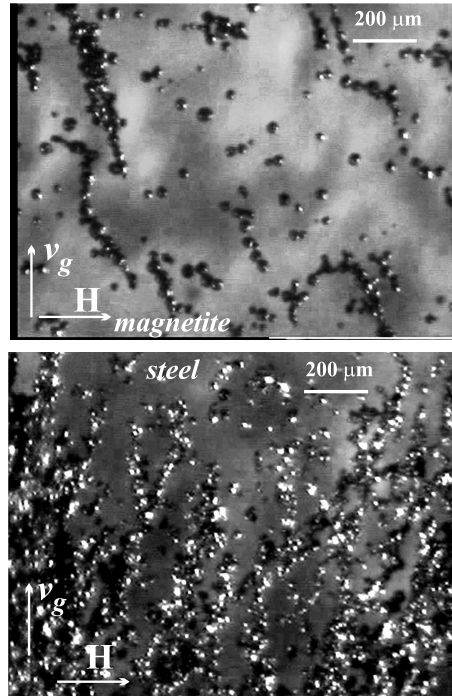
FIG. 16: Optical microscope images of the steel and magnetite particles taken from the magnetofluidized bed ($H \simeq 4$ kA/m).